

Co-Registration of Two DEMs: Impacts on Forest Height Estimation from SRTM and NED at Mountainous Areas

Wenjian Ni, Guoqing Sun, Zhiyu Zhang, Zhifeng Guo, and Yating He

Abstract—The digital elevation model from the Shuttle Radar Topography Mission (SRTM) and the National Elevation Dataset (NED) have been used to estimate the forest canopy height. Most of such studies have been conducted over flat areas; the method performance has not been carefully examined over mountainous areas. This study, which is conducted over two mountainous test sites located in California and New Hampshire, reveals that the co-registration of these two digital elevation models (DEMs) is crucial to ensuring the quality of the results. The image co-registration method used in interferometric SAR processing is adapted to the co-registration of two DEMs. The forest canopy height from the Laser Vegetation Imaging Sensor (LVIS) is used as the reference data. The results showed that the misregistration between SRTM and NED was very obvious at both test sites. After the co-registration, the R^2 of the correlation between the height of the C-band scattering phase center derived from SRTM minus NED and the forest canopy height derived from LVIS data was improved from 0.19 to 0.51, and RMSE was reduced from 16.4 m to 6.8 m for slope up to 55° at the California test site, while the R^2 was improved from 0.39 to 0.57 and RMSE was reduced from 5.4 m to 3.6 m for slopes up to 45° at the New Hampshire test site. The influences of data resolution and terrain slopes were also investigated. The results showed that reducing the data resolution by spatial averaging could not reduce the influence of DEM misregistration.

Index Terms—Digital elevation model (DEM) co-registration, forest canopy height, mountain, National Elevation Dataset (NED), Shuttle Radar Topography Mission (SRTM).

I. INTRODUCTION

FOREST canopy height is an important parameter for forest management and forest ecosystem studies. The digital elevation model from the Shuttle Radar Topography Mission (SRTM) and National Elevation Dataset (NED) have been used to estimate the forest canopy height. Kellendorfer *et al.* [1] studied the extraction of the forest canopy height from SRTM using the NED. Simard *et al.* [2] explored the mapping

Manuscript received November 4, 2012; revised February 15, 2013; accepted March 7, 2013. This work was supported in part by the China MOST 863 Program (2012AA12A306); the National Natural Science Foundation of China under Grants 41001208, 40971203, and 41171283; the Strategic Priority Research Program, Climate Change: Carbon Budget and Related Issues, Chinese Academy of Sciences, under Grant XDA05050100; and the NASA Terrestrial Ecology Program (NNX09AG66G). (Corresponding author: Z. Zhang).

W. Ni, Z. Zhang and Z. Guo are with State Key Laboratory of Remote Sensing Science, Jointly Sponsored by the Institute of Remote Sensing Applications of the Chinese Academy of Sciences and Beijing Normal University, Beijing 100101, China (e-mail: zhangzy@irsa.ac.cn).

G. Sun is with the University of Maryland, College Park, MD 20742 USA. Y. He is with the Institute of Geographic Sciences and Natural Resources Research, Chinese Academy of Sciences, Beijing 100101, China.

Color versions of one or more of the figures in this paper are available online at <http://ieeexplore.ieee.org>.

Digital Object Identifier 10.1109/LGRS.2013.2255580

of mangrove forest height in the Everglades National Park using SRTM calibrated by U.S. Geological Survey (USGS) digital terrain model (DEM) and airborne Light Detection and Ranging (LIDAR). The use of SRTM and NED data to estimate forest canopy height is promising because SRTM is derived from interferometric synthetic aperture radar (InSAR) data, which is sensitive to the vertical distributions of forest components. Meanwhile, SRTM is based on the C-band, which is mainly scattered by forest canopy. Most of the studies to date have been mainly conducted over relatively flat areas [1], [2]. The co-registration between SRTM and NED were not specially considered, especially over mountainous areas. Van Niel *et al.* [3] found that the error caused by the subpixel misregistration of two DEMs was greater than or equal to the true difference between the two models. However, the continuous nature of DEM makes co-registration difficult because it is difficult to find accurate control points, which are needed for traditional co-registration approaches. Nuth and Käab [4] tried to rectify the errors caused by the misregistration of DEMs using regression analysis between error and slope as well as aspects. Van Niel *et al.* [3] proposed a modified method based on the work in [5] and [6]. An initial registration was first made using ground control points. Next, one DEM was shifted along the x and y directions in increments of 1/25th of a grid cell. The best registration was determined by the shift that produced the highest spatial autocorrelation. It is clear that this method can only rectify the misregistration caused by the relative horizontal movement, and the accuracy is determined by the shift step. The misregistration induced by rotation, skew, and scaling cannot be rectified.

In this letter, a method for the co-registration of two DEMs is firstly proposed. Two ground-range SAR images are simulated from two DEMs by assuming that the backscattering from the surface is determined by the cosine of the local radar incidence angle. The co-registration coefficients are estimated by using the common points recognized from the two simulated SAR image. Then the co-registration coefficients are employed to project one DEM into the other. The effects of co-registration on the forest canopy height estimation from SRTM and NED are further investigated over two mountainous test sites. The forest canopy height from the Laser Vegetation Imaging Sensor (LVIS) is taken as the reference data because LIDAR data are believed to be direct measurements of the forest vertical structure [7]. The correlation between the difference of SRTM and NED (SRTM-NED) and forest canopy height is analyzed under different terrain slopes and data resolutions.

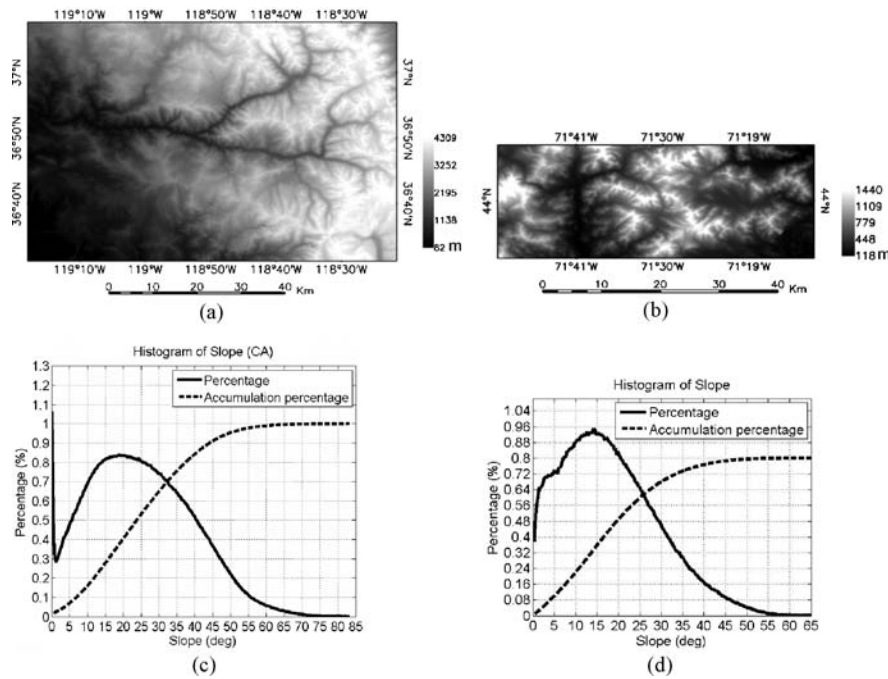


Fig. 1. Location and terrain conditions of the California (CA) and New Hampshire (NH) test sites. (a) NED of the California site. (b) NED of the New Hampshire site. (c) Histogram of the terrain slope of (a). (d) Histogram of the terrain slope of (b). The vertical grid is 10% for the accumulation percentage in (c) and (d).

II. TEST SITES AND DATA

A. Test Sites

Two test sites in the U.S. are used in this letter. The first ($36^{\circ}50'N$, $118^{\circ}50'W$) is located between Tollhouse and Independence in California (CA), and the second ($44^{\circ}0'N$, $71^{\circ}30'W$) is located between Warren and Conway in New Hampshire (NH), as shown in Fig. 1. Fig. 1(a) is the 1 arc-second NED of the CA site downloaded from USGS, whereas Fig. 1(b) is the corresponding NED of the NH site. These data indicate that the elevation ranges from 82 to 4309 m at the CA site and from 118 to 1440 m at the NH site. Fig. 1(c) shows the histogram of slopes from Fig. 1(a): 40% of the area has slopes of less than 20° , and 10% has slopes of greater than 45° . Fig. 1(d) shows the histogram of slopes from Fig. 1(b): 30% of the area has slopes of less than 10° , and 10% has slopes of greater than 35° .

B. Data

The SRTM instrument consisted of a C-band radar and additional antenna to form an interferometer with a 60-m baseline. It flew onboard the Space Shuttle Endeavour during an 11-day mission in February 2000. The SRTM data are distributed into two levels: SRTM-1, with data sampled in 1 arc-second intervals in latitude and longitude, and SRTM-3, with data sampled in 3 arc-second intervals. SRTM-1 data were downloaded from USGS (<http://dds.cr.usgs.gov/srtm/>) and used in this letter. The elevations are in meters, referenced to the WGS84/EGM96 geoid. The SRTM data were transformed to the ellipsoid surface of GRS80 using the GEOTRANS software developed by the National Geospatial-Intelligence Agency.

NED is distributed in geographic coordinates in units of decimal degrees by USGS. Its horizontal reference is the North American Datum of 1983 (NAD 83), and its vertical reference

is the North American Vertical Datum of 1988 (NAVD 88). The NED data were transformed to the ellipsoid surface of GRS80 using GEOID12, which was developed by the National Geodetic Survey (NGS). The relative vertical accuracy of the 1 arc-second NED versus the reference geodetic points was reported as 2.44 m, whereas [8] reported a mean variation of up to 5 m compared with LIDAR ground DEM.

NASA's LVIS is an airborne laser altimeter system designed, developed, and operated by the Laser Remote Sensing Laboratory at the Goddard Space Flight Center. The LVIS data used in this letter were acquired on Sept. 21st, 2008, in CA and on Aug. 1st, 2009, in NH using a 20-m footprint. LVIS ground elevation data include location (latitude/longitude), ground surface elevation, and the heights of the energy quartiles (relative height to ground surface; RH25, RH50, RH75, and RH100) where 25%, 50%, 75%, and 100% of the waveform energy occur. The elevation is referred to WGS-84 (i.e., GRS80) ellipsoid. The quartile heights are the relative direct measurements of the vertical profile of canopy components. The RH100 of LVIS data for the study area was rasterized to an image with 1 arc-second \times 1 arc-second pixels. The RH100 and RH50 of footprints located within a pixel were averaged separately to be the value of the pixel. The pixels having no footprints were masked out in the analysis.

III. METHOD

A. Image Co-Registration Algorithm

The image needing to be resampled is referred to as the slave image, whereas the other image is referred to as the master image. Automatic co-registration of SAR images is a common procedure in InSAR data processing [9]. It models the misregistration between master and slave images caused

by horizontal translation, scale, skew, and rotation as

$$\begin{bmatrix} x_m \\ y_m \end{bmatrix} = A \begin{bmatrix} x_s \\ y_s \end{bmatrix} + \begin{bmatrix} x_0 \\ y_0 \end{bmatrix}, \quad A = \begin{bmatrix} \cos \varphi & \sin \varphi \\ -\sin \varphi & \cos \varphi \end{bmatrix} \begin{bmatrix} k_x & w \\ 0 & k_y \end{bmatrix} \quad (1)$$

where $(x_0, y_0)^T$ is the horizontal translation vector, (k_x, k_y) is the scale factors along the sample and line directions, w is the skew term, and φ is the rotation angle. There are six transformation parameters that must be determined. $(x_m, y_m)^T$ are the center coordinates of a chip in the master image, whereas $(x_s, y_s)^T$ are the center coordinates of a chip in the slave image having maximum correlation with the master chip.

The common points (control points) of these two images were searched automatically, after which the point qualities were screened based on the signal-to-noise ratio. To achieve successful co-registration, the number of common points should be much more than the number of parameters to be determined. The resultantly over-determined system of linear equations can be solved using the least squares method.

B. Co-Registration of DEMs

Two ground-range SAR images are simulated from two DEMs by assuming that the backscattering from the surface is determined by the cosine of the local radar incidence angle. Assuming that a left-looking SAR flew along a straight line from north to south with a specified incidence angle α (e.g., 40°), the formula for the calculation of local incidence is as follows [10]:

$$\cos(\theta) = \sin(\alpha_s) \sin(\alpha) \cos(\beta - \beta_s) + \cos(\alpha_s) \cos(\alpha) \quad (2)$$

where θ is the local incidence angle; α and β are the incidence zenith and azimuthal angle of SAR, respectively; and α_s and β_s are the local slope and aspect angle from DEM, respectively. According to the flight assumption, $\alpha = 40^\circ$ and $\beta = 90^\circ$. Two images of the cosine of local incidence angle can be produced from two DEMs using equation (2). Their co-registration parameters can be calculated using the algorithm described in previous section by using one as the master image and the other as the slave image. The co-registration can be accomplished by resampling the slave DEM to the master DEM using the estimated parameters.

C. Results Validation

The LIDAR data are the direct measurements of the vegetation vertical structures. In this letter, RH50 from LVIS data is used to determine the forested area. The pixels having RH50 higher than 0.5 m are taken as forested pixels. RH100 from LVIS serves as a reference of forest canopy height. The correlation between SRTM-NED and forest canopy height is investigated before and after the co-registration of SRTM and NED. Kellndorfer *et al.* [1] reported that averaging at least 20 SRTM pixels per observation provides better results. Therefore, the investigation is made at several resolutions from 1 arc-second to 5 arc-seconds to explore the resolution effect. Moreover, the slope effect is also considered in the comparison. The analyses are conducted on different slope intervals in 5° increments.

IV. RESULTS

The overlay flashing display of cosine images of local incidence angle from SRTM and NED at the CA site shows

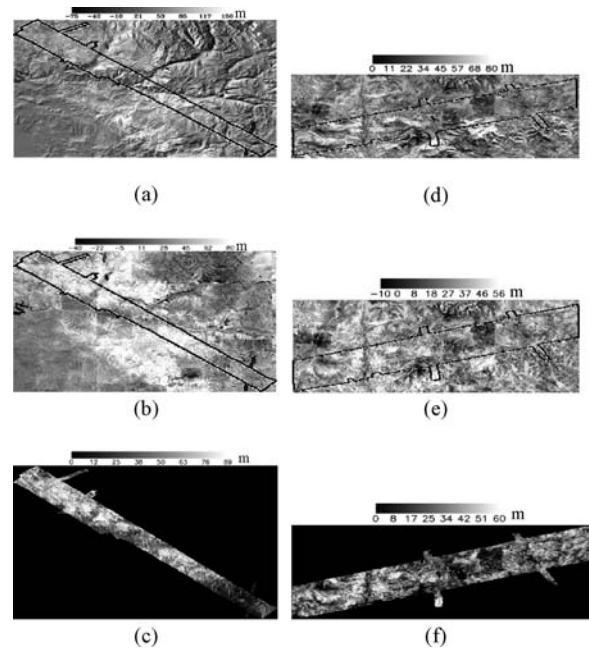


Fig. 2. Differences between SRTM and NED before and after the co-registration of SRTM and NED. (a) Difference between original SRTM and NED at CA. (b) Difference between registered SRTM and NED at CA. (c) RH100 from LVIS data at CA. (d) Difference between original SRTM and NED at NH. (e) Difference between registered SRTM and NED at NH. (f) RH100 from LVIS data at NH. The polygons in (a), (b), (d), and (e) are the area covered by LVIS data

that the displacements between SRTM and NED are different in different parts of the area. Therefore, they must be co-registered piece by piece. The piece size is specified as 500 arc-seconds by 500 arc-seconds. For the NH site, a horizontal line is discovered in the image derived from (2), dividing the SRTM data into two parts. The overlay flashing display shows that the deformations are different for each of the two parts of the SRTM data relative to NED. Therefore, the two parts of the SRTM data were registered separately to NED, and the mosaic was made after registration at the NH site.

Fig. 2 shows the difference images between SRTM and NED before and after the co-registration of SRTM and NED. Fig. 2(a)–(c) corresponds to the CA site, whereas Fig. 2(d)–(f) corresponds to the NH site. Fig. 2(a) and (d) are the difference images between the original SRTM and NED. The terrain effects are very clear in these two images. Fig. 2(b) and (e) are the difference images between the co-registered SRTM and NED, wherein the terrain effects caused by misregistration between SRTM and NED are almost removed. Fig. 2(c) and (f) are the RH100 from LVIS data. The black polygons in Fig. 2(a), (b), (d), and (e) are the areas corresponding to the LVIS coverage. It can be seen that the difference images resemble the RH100 images better after co-registration than before co-registration. Table I shows the estimated transformation parameters of SRTM relative to NED. “Upper part” and “lower part” refer to the NH site, while the rest are for the CA site. The CA site is divided into four rows and six columns in the co-registration. Fig. 3 depicts the horizontal displacement of the different pieces of SRTM relative to NED. R_i and C_j stand for the i^{th} row and j^{th} column, respectively. The arrows are drawn in the unit of pixel size, and their lengths represent the relative magnitudes of the displacement. The displacement value and direction differ by piece.

TABLE I
AFFINE PARAMETERS FOR CO-REGISTERING THE UPPER
AND LOWER PARTS OF SRTM TO NED*

Part	Skew	Scale vectors		Rotation (deg)
		Longitude direction	Latitude direction	
Upper part	-8.87E-05	0.9999	1.0002	-4.0E-04
Lower part	-3.2E-04	1.0001	0.9989	-2.3E-03
R1C1	8.34E-05	0.9999	0.9996	-8.83E-03
R1C2	4.82E-04	1.0003	0.9970	-3.09E-02
R1C3	2.28E-03	0.9995	0.9971	5.16E-02
R1C4	-2.25E-04	1.0000	0.9998	4.00E-03
R1C5	2.60E-03	1.0008	0.9999	1.79E-02
R1C6	1.55E-03	1.0001	1.0001	7.36E-03
R2C1	1.59E-03	0.9997	0.9993	5.95E-02
R2C2	3.32E-04	1.0000	0.9997	7.33E-03
R2C3	-1.39E-03	0.9996	1.0018	-2.40E-02
R2C4	1.27E-03	0.9996	1.0023	5.50E-02
R2C5	1.01E-03	0.9999	1.0006	5.20E-02
R2C6	1.11E-04	1.0000	0.9995	-1.31E-02
R3C1	-1.33E-03	0.9995	1.0001	-3.49E-02
R3C2	-5.96E-04	0.9997	1.0000	7.86E-03
R3C3	-2.37E-04	1.0001	0.9975	-1.45E-02
R3C4	8.45E-04	0.9994	0.9982	2.74E-02
R3C5	-6.15E-05	1.0000	1.0001	-5.58E-03
R3C6	-5.88E-05	0.9994	1.0003	-5.62E-03
R4C1	6.02E-04	0.9998	1.0001	-2.36E-03
R4C2	8.22E-04	0.9997	1.0000	2.20E-04
R4C3	2.38E-04	0.9996	1.0001	2.48E-02
R4C4	-1.82E-03	0.9995	1.0010	-6.28E-02
R4C5	-1.97E-04	0.9989	0.9999	2.53E-02
R4C6	-1.33E-03	0.9999	1.0007	-6.16E-02

* Upper part and lower part correspond to the NH site, whereas the rest are for the CA site. The area of the CA site is divided into 4 rows and 6 columns in the co-registration. RiCj: the piece of the i^{th} row and j^{th} column. The horizontal respectively.

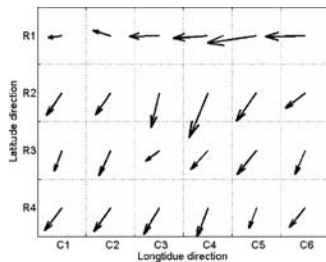


Fig. 3. Horizontal translation of SRTM relative to NED. The length of the arrows represents relative magnitude of the displacement

Fig. 4 presents the scatter-plot of SRTM-NED against RH100. Fig. 4(a) and (b) corresponds to the CA site, whereas Fig. 4(c) and (d) corresponds to the NH site. The co-registration improves the R^2 from 0.19 to 0.51 and reduces the RMSE from 16.4 m to 6.8 m at the CA site for slopes up to 55° . For NH, the R^2 is improved from 0.39 to 0.57 and the RMSE is reduced from 5.4 m to 3.6 m by the DEMs co-registration for slopes up to 45° .

Fig. 5 shows the correlation between SRTM-NED and forest canopy height under different data resolutions and terrain slope intervals before and after the co-registration of SRTM and NED. Fig. 5(a) and (b) are, respectively, the R^2 and RMSE of linear regression between SRTM-NED and RH100 under different slope ranges at the CA site, whereas Fig. 5(c) and (d) corresponds to the NH site. Fig. 5 further confirms the importance of the co-registration of SRTM and NED over mountainous areas. The correlation of SRTM-NED with forest canopy height is obviously improved under all

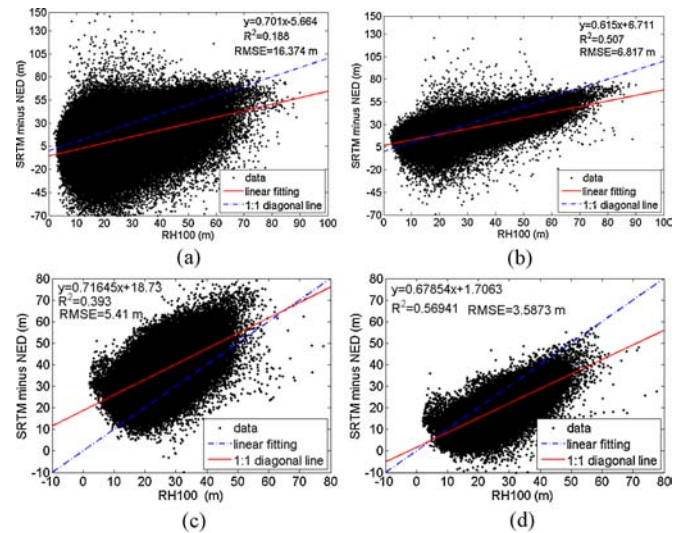


Fig. 4. Scatter plots of SRTM-NED versus RH100 (a) before registration (CA site), (b) after registration (CA site), (c) before registration (NH site), and (d) after registration (NH site).

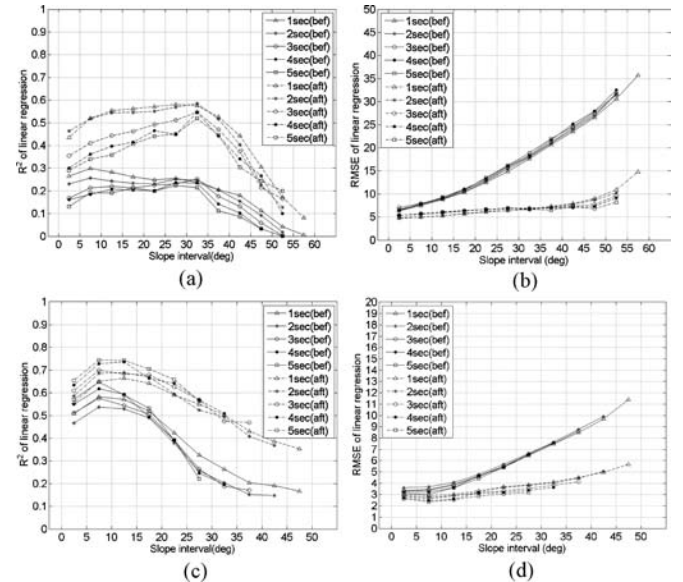


Fig. 5. Correlation between SRTM-NED and forest canopy height under different data resolutions and terrain slope intervals before and after the co-registration of SRTM and NED. (a) and (b) show the R^2 and RMSE for the CA site, respectively, whereas (c) and (d) show the R^2 and RMSE for the NH site, respectively.

data resolutions and terrain slopes after co-registration. The R^2 is approximately 0.5 for forest located on slopes up to 35° at the CA site.

V. DISCUSSION

The difference between two DEMs is very sensitive to misregistration for areas with significant relief. A shift of a fraction of a pixel may cause significant changes in the elevation difference between two DEMs if the pixel is on a slope and the shift is in the direction of the slope. As shown in this letter, this error cannot be removed by reducing spatial resolution because all pixels on a slope are affected due to misregistration. Supposing there is a ridge from north to south, a displacement occurred due to the movement of SRTM to the west of NED with a magnitude of a fraction

of a pixel. For pixels located on the west slope, the elevation differences between SRTM and NED should be larger than their true value. For pixels located on the east slope, their elevation differences should be smaller than their true value. This error cannot be eliminated by averaging of several pixels unless the final pixel size is so large that it can cover both the west and east slopes.

Fig. 4(c) and (d) shows that there are some negative values in SRTM-NED after co-registration. These negative pixels are always scattered along steep, narrow valleys over mountainous areas. The changes in gradient and aspect are sharper over steep, narrow valleys than slopes. The sensitivity of the InSAR phase to the frequent elevation changes may not be high enough due to the accuracy of the InSAR phase measurement. Alternatively, the misregistration over steep, narrow valleys may be different from that of other areas.

Although a SAR is assumed to fly over the terrain covered by DEMs when calculating the local incidence angle, the calculation is conducted in the original DEM coordinate (ground range). There is no transformation or projection to slant range geometry. Therefore, the inherent distortions of SAR images, such as foreshortening and layover, will not appear in the local incidence angle image. The SAR is supposed to be left-looking and to fly from north to south. Under this condition, the upper left corner of simulated image corresponds to the northwest corner of the DEM. The incidence angle is not necessarily 40° ; it can be 20° , 30° , or any other value from 0° to 90° as long as the local incidence angles of two DEMs are calculated using the same parameters.

The co-registration method adopted here can consider the misregistration of DEMs caused by translation, rotation, scale, and skew. The co-registration is mainly based on the recognition of common terrain features. The more terrain features found, the better the success of the registration. Occasional failure occurred only for very flat areas with a near complete absence of terrain features. However, in practice, it is not critical to perform co-registration over these very flat areas. Another advantage of the proposed method is that it enables users to check the misregistration visually by overlay the flashing display, which can help users divide the image into sub-images for piecemeal co-registration, as done in this letter.

Table I and Fig. 3 show that horizontal translation is the most influential parameter. However, the other parameters can not be neglected. Near the edge of a $500 \text{ pixel} \times 500 \text{ pixel}$ sub-image, equation (1) shows that a 0.01° rotation can cause the displacement of 0.087 pixels, a scale of 0.9998 or 1.0002 can cause the movement of 0.1 pixels, and a skew of ± 0.0002 can cause the displacement of 0.1 pixels. The parameters given in Table I are equal to or greater than the typical values of these parameters, which further demonstrates that skew, rotation, and scale factors also must be considered in the DEM co-registration.

The co-registration method proposed herein is imposed on SRTM and NED data for the forest canopy height estimation. In fact, the comparison of DEMs has many applications in geography, such as to assess the vertical and horizontal accuracies of new DEMs, as performed by Hofton *et al.* [5], to measure vegetation height, as performed by Simard *et al.* [2], and to estimate glacier volume change, as performed by Berthier *et al.* [11]. The most important prerequisite of these applications is the accurate co-registration of DEMs. The method proposed in this letter can tolerate some differences

between the two DEMs to be co-registered as long as their basic terrain features are similar. For example, the SRTM and NED data have some slightly different features in forested areas. The elevation difference of these two DEMs ranges within several tens of meters, as shown in Fig. 4. The proposed method should be applicable for other DEMs whose difference is in similar ranges.

VI. CONCLUSION

The forest canopy height estimation over mountainous areas using SRTM and NED data were investigated. The research was conducted at two mountainous test sites. An automatic co-registration method for SRTM and NED was proposed. The results at both sites showed that the method was effective and that misregistration must be considered in the forest canopy height estimation over mountainous terrain. The correlation between SRTM-NED and forest canopy height information from LVIS was obviously improved under all data resolutions and slope intervals. It is feasible to retrieve forest canopy heights over mountainous areas using SRTM and NED for slopes up to 55° .

ACKNOWLEDGMENT

The LVIS datasets were provided by the LVIS team in the Laser Remote Sensing Branch, NASA Goddard Space Flight Center, with support from the University of Maryland, College Park. The authors would like to give thanks to them.

REFERENCES

- [1] J. Kelndorfer, W. Walker, L. Pierce, C. Dobson, J. A. Fites, C. Hunsaker, J. Vona, and M. Clutter, "Vegetation height estimation from shuttle radar topography mission and national elevation datasets," *Remote Sens. Environ.*, vol. 93, no. 3, pp. 339–358, 2004.
- [2] M. Simard, K. Q. Zhang, V. H. Rivera-Monroy, M. S. Ross, P. L. Ruiz, E. Castaneda-Moya, R. R. Twilley, and E. Rodriguez, "Mapping height and biomass of mangrove forests in Everglades National Park with SRTM elevation data," *Photogram. Eng. Remote Sens.*, vol. 72, no. 3, pp. 299–311, 2006.
- [3] T. G. Van Niel, T. R. McVicar, L. T. Li, J. C. Gallant, and Q. K. Yang, "The impact of misregistration on SRTM and DEM image differences," *Remote Sens. Environ.*, vol. 112, no. 5, pp. 2430–2442, 2008.
- [4] C. Nuth and A. Käab, "Co-registration and bias corrections of satellite elevation data sets for quantifying glacier thickness change," *Cryosphere*, vol. 5, no. 1, pp. 271–290, 2011.
- [5] M. Hofton, R. Dubayah, J. B. Blair, and D. Rabine, "Validation of SRTM elevations over vegetated and non-vegetated terrain using medium footprint lidar," *Photogram. Eng. Remote Sens.*, vol. 72, no. 3, pp. 279–285, 2006.
- [6] E. Rodriguez, C. S. Morris, and J. E. Belz, "A global assessment of the SRTM performance," *Photogram. Eng. Remote Sens.*, vol. 72, no. 3, pp. 249–260, 2006.
- [7] M. A. Lefsky, M. Keller, Y. Pang, P. B. De Camargo, and M. O. Hunter, "Revised method for forest canopy height estimation from Geoscience Laser Altimeter System waveforms," *J. Appl. Remote Sens.*, vol. 1, no. 1, p. 013537, 2007.
- [8] L. Kenyi, R. Dubayah, M. Hofton, and M. Schardt, "Comparative analysis of SRTM-NED vegetation canopy height to LIDAR-derived vegetation canopy metrics," *Int. J. Remote Sens.*, vol. 30, no. 11, pp. 2797–2811, 2009.
- [9] S. M. Buckley, "Radar interferometry measurement of land subsidence," Ph.D. dissertation, Univ. Texas, Austin, TX, USA, 2000.
- [10] G. Sun, K. J. Ranson, and V. I. Kharuk, "Radiometric slope correction for forest biomass estimation from SAR data in the Western Sayani Mountains, Siberia," *Remote Sens. Environ.*, vol. 79, no. 2, pp. 279–287, 2002.
- [11] E. Berthier, Y. Arnaud, C. Vincent, and F. Remy, "Biases of SRTM in high-mountain areas: Implications for the monitoring of glacier volume changes," *Geophys. Res. Lett.*, vol. 33, no. 8, pp. L08502 (1–5), 2006.